Environmental Science Nano

ROYAL SOCIETY OF CHEMISTRY

PAPER

View Article Online
View Journal | View Issue

Cite this: *Environ. Sci.: Nano*, 2024, 11, 2683

Bio-based carbon foams assembled with Fe nanoparticles for simultaneous remediation of As, Hg and PAHs in co-contaminated industrial soils†

I. Janeiro-Tato,[ab] E. Rodríguez,[a] M. A. Lopez-Anton,[*a] D. Baragaño,[a] L. Arrojo,[a] P. Parra-Benito,[a] A. I. Peláez[bc] and J. R. Gallego[d]

Received 11th December 2023,
Accepted 22nd April 2024

DOI: 10.1039/d3en00927k

rsc.li/es-nano

Although numerous amendments show well-defined efficiencies for the remediation of soils contaminated with metals, metalloids, and organic compounds separately, few technologies have been developed capable of remediating multi-contaminated soils. In this study, carbon foams prepared from sucrose with and without impregnation with iron species were applied at a 10% dose to immobilize As on two industrial soils co-contaminated with Hg and PAHs. The results obtained by the toxicity characteristic leaching procedure (TCLP) test showed that the application of the sucrose foam loaded with iron nanoparticles decreased the leachability of As in both soils (15–20%), being statistically significant only in the case of T soil, whereas the availability of Hg was considerably reduced with both sucrose foams (50–60%). With regard to the bioavailable fraction of PAHs determined by a non-exhaustive technique, the treatment with the carbon foams caused a significant decrease of PAH content (90–96%). The macro-, meso- and microporosity of the sucrose foams (S_{BET} ~300 m^2 g^{-1}), their structure based on condensed aromatic sheets, and the possibility of depositing iron nanoparticles on their surface (FeOOH and Fe_3O_4) make them promising new amendments for the sustainable remediation of multi-contaminated soils.

Environmental significance

Mercury, arsenic and polycyclic aromatic hydrocarbons (PAHs) are well known for their toxic effects on human health. Most of these organic and inorganic pollutants come from anthropogenic sources, causing soil deterioration. Therefore, excessive levels of these toxic pollutants in soils are of great concern both for the environment and for their subsequent transfer to the human food chain. In this study, a new sustainable material based on a carbon foam has been developed capable of remediating multi-contaminated soils, a task that is often not easy to carry out. The work is approached not only from the point of view of reducing the mobility of these contaminants but also from the study of their bioavailability. Furthermore, the application of the novel nanocomposite developed immobilizes the contaminants without altering the natural levels of Fe(II) in the soil, which avoids the drawbacks of some materials developed to date.

1. Introduction

According to the European Environment Agency (EEA), rapid and generalized urbanization and industrialization cause an environmental imbalance, with the soil being one of the most affected compartments. Soil pollution has been identified as the third most important threat to Europe,[1] with more than 10 million contaminated sites worldwide.[2] Although some elements and compounds are naturally present in the soil, most of the organic and inorganic pollutants come from anthropogenic sources.[3,4] High concentrations of metal(loid)s and organic contaminants can cause deterioration of the physicochemical properties and biological function of the soil.[5] Excessive levels of toxic pollutants in soils are of great concern both for the environment and for their subsequent transfer to the human food chain.[6] Metal(loid)s such as Hg and As are well known for their toxic effects on the kidney and nervous system,[7] whereas organic pollutants such as polycyclic aromatic hydrocarbons (PAHs) are registered as priority pollutants due to their persistent, toxic, genotoxic and carcinogenic nature.[8]

[a] *Instituto de Ciencia y Tecnología del Carbono, INCAR-CSIC, C/Francisco Pintado Fe, 26, 33011 Oviedo, Spain. E-mail: marian@incar.csic.es; Tel: Phone: +34 985 118959*
[b] *Area of Microbiology, Department of Functional Biology and Environmental Biogeochemistry and Raw Materials Group, University of Oviedo, Oviedo, Spain*
[c] *University Institute of Biotechnology of Asturias (IUBA), University of Oviedo, Oviedo, Spain*
[d] *INDUROT and Environmental Biogeochemistry and Raw Materials Group, University of Oviedo, Mieres, Spain*

† Electronic supplementary information (ESI) available. See DOI: https://doi.org/10.1039/d3en00927k

The intense industrial and mining activity that has taken place in many regions for decades has left many sites affected by a complex mix of pollutants. In many cases, such places are situated close to urban and peri-urban areas.[9,10] The mix of contaminants poses a challenge for *in situ* remediation.

The mobility of the pollutants depends on their chemical speciation which is mainly a function of pH and redox potential of soil. In addition to the knowledge of speciation, the analysis of the bioavailable fraction of each type of contaminant will be essential to assess environmental risk and to predict bioremediation efficiency.[11]

Investigations on the remediation of both organic and inorganic pollutants (individually) are large. Single contamination can be effectively treated with the help of immobilizing agents such as nanomaterials.[12] However, remediation of co-contaminated soils is more complex.[13,14] The interaction between organic and inorganic compounds may alter the solubility and bioavailability of pollutants. In addition, the adsorbed pollutants can be affected by competition for the active binding sites.[15] *In situ* immobilization uses iron oxides and zero valence iron nanoparticles (nZVI) which are remarkable for their high capacity to immobilize As in soils.[16] A decrease of 90% in As availability by toxicity characteristic leaching procedure (TCLP) test was achieved at a dose of 2% nZVI.[17] The mechanism of immobilization may involve adsorption and coprecipitation reactions and formation of secondary minerals.[18,19] However, this type of amendments presents, among others, the risk of an increase in the availability of certain metals such as Cu.[20,21] On the other hand, historical mining and processing have led to multiple soils contaminated not only with As but also with heavy metals such as Hg, which requires various approaches for their remediation.[22,23] Unlike As, the immobilization of mercury by *in situ* stabilization is a technology still under development. The addition of sulfur-containing ligands is one the most stabilizing methods used to immobilize mercury. Treatments with iron sulfide nanoparticles and biochar modified with elemental sulfur have been reported to reduce the leachability of mercury up to 95–99% with treatment dosages of 1–5% in TCLP leachates.[24,25] Graphene oxide/Fe–Mn composite and nZVI were also employed as amendments for mercury immobilization, reaching satisfactory results.[26,27] The leachability of mercury was significantly reduced by 90–99% at dosages of 0.4% and 0.8% composite and 50–80% at a dose of 2.5% nZVI in batch leaching tests. Nevertheless, the potential effects of the nanoparticles on the environment and an increase in the volume of waste must be taken into consideration when this type of amendment is applied. Organic pollutants may also be present in many of these abandoned sites along with As.[9,28]

Although some studies have focused on both metal(loid)s and organic pollutants,[29–31] remediation technologies that can stabilize both types of contaminants have not yet been thoroughly evaluated. Nanoscale materials have been evaluated for the immobilization of organic pollutants in contaminated soils; in particular, activated carbon nanoparticles and magnetite nanoparticles may adsorb PAHs from soil, lowering their bioavailability and reducing their concentration due to the sorption process.[32] Iron-based compounds have also showed to be effective in simultaneously immobilizing As and PAHs.[28] However, most studies are based on a combination of remediation technologies (microbial–plant or electrokinetics–biostimulation combination, chemical oxidation–bioremediation)[29,30,33,34] whose efficiencies depend on the type of plant, metals, *etc.*, and in many cases they are costly and laborious techniques. Therefore, the remediation of contaminated soils is an unquestionable requirement that must be addressed from different fronts.

The innovative content of this study covers two main aspects: (1) how to address the problem of immobilization of As when metals, such as Hg, or organic contaminants, such as PAHs, are also present, and (2) the development of a new amendment to solve the problem, both approaches framed within natural and environmentally sustainable solutions. Although carbon foams prepared using coal as a precursor have previously been used to reduce the availability of Hg and As achieving efficiencies of 75–100%,[35,36] the fact that the carbon foams developed in this study use a low-cost sustainable precursor and that their preparation involves a low energy cost make them an economically competitive product compared to other carbon foams developed in the market.[37] Furthermore, the use of this new amendment could fill a gap in this field, sometimes difficult to cover with biochars, such as the remediation of soils contaminated with both metals and metalloids.

In this study, the use of a carbon foam obtained from a bio-precursor (sucrose) is proposed as a novel sustainable approach for the remediation of soils co-contaminated with PAHs, Hg and As. The objective of the study was to evaluate not only the efficiency of a new amendment for the immobilization of several contaminants through leaching tests but also the bioavailability of PAHs through extraction techniques. A better understanding of this issue is helpful to elucidate the interaction mechanism and optimize strategies for *in situ* remediation.

2. Materials and methods

2.1 Soil samples and analysis methods

For the development of this work, two soils were used, one from an abandoned Hg mining-metallurgy site, El Terronal mine (T soil), and another from an old ammonia factory (M soil) from two regions in the north and south of Spain, respectively. The soils are located in areas of high industrial activity with high levels of contamination by As and Hg, and As and PAHs, respectively.[28,38]

The pH and electrical conductivity (EC) of the soils were determined in a suspension of 1 g of soil and 2.5 ml Milli-Q water.

The total content of As in the soils was determined by inductively coupled plasma mass spectrometry (ICP-MS) after digestion with 3 : 1 : 0.5 (v/v/v) concentrated HCl/HNO_3/HF in a microwave oven, whereas the total content of Hg was directly determined using an AMA 254 automatic mercury analyzer.

The mobility of As and Hg in the soils was evaluated by using the toxicity characteristic leaching procedure (TCLP) test.[39] Additionally, the availability of As and Hg was also assessed using two specific sequential extraction methods proposed by Wenzel *et al.*[40] and the United States Environmental Protection Agency (USEPA) Method 3200,[41] respectively. The adopted sequential extraction method proposed by Wenzel *et al.* provides the following fractions: non-specifically sorbed As, specifically sorbed As, amorphous hydrous oxide-bound As, crystalline hydrous oxide-bound As and residual As. In turn, USEPA Method 3200 provides mobile Hg, semi-mobile Hg and non-mobile Hg. The resultant concentrations of As and Hg were analysed by ICP-MS and AMA 254, respectively.

The total concentration of 16 PAHs, designated by the USEPA as priority pollutants, was determined by gas chromatography mass spectrometry (GC-MS) after an exhaustive extraction technique. The analysis by GC-MS is detailed in the ESI.† The extraction was carried out using an acetone–hexane mixture in an orbital shaker, following a procedure similar to that of Beesley *et al.*[42,43] The resultant solution was filtered and subsequently concentrated by rotary evaporation.

The bioavailable fraction of PAHs was determined by a non-exhaustive technique using hydroxypropyl-β-cyclodextrin (HPCD). This term defines the bioavailable amount of contaminants that can be desorbed over time (not in a given moment of time).[44] Briefly, 3 g of soil were mixed with a 45 ml solution of 60 mM HPCD in deionised water and shaken for 20 h on an orbital shaker at 250 rpm.[42,43] After extraction, the mixture was centrifuged and the supernatant was discarded. To determine the PAH concentration remaining in the soil after HPCD extraction, the resultant soil was then subjected to the acetone–hexane extraction described above. After concentration and clean-up, the extract was analysed by GC-MS.

The results of the HPCD extraction were divided into two fractions, bioavailable and residual. The concentration remaining in the soil after HPCD extraction represents the residual concentration measured (C_R). Thus, the bioavailable concentration (C_B) was calculated by subtracting the residual concentration (C_R) from the total concentration (C_T). Both total and HPCD extractions were carried out in triplicate and included deuterated PAH recovery standard (20 μl of pyrene-d10 from a 100 μg mL^{-1} stock solution). The recoveries ranged from 75% to 110% for individual PAHs.

2.2 Soil amendment and characterization methods

Sucrose foams (SFs) were prepared by mixing 16 g of sucrose with 0.32 g of iron nitrate nonahydrate ($Fe(NO_3)_3{\cdot}9H_2O$), which acts as a foaming enhancer and activating agent, in 5 ml of Milli-Q water. The mixture was concentrated on a hot plate until it became a dark viscous resin and foamed afterwards in an air oven at 300 °C for 3 h at a heating rate of 2 °C min^{-1}. The resultant foams were ground and carbonized for 2 h at 800 °C in a horizontal tubular furnace under an argon flow of 50 ml min^{-1} at a heating rate of 5 °C min^{-1}. After that, the final foam was ground to 0.2–0.5 mm. The SF was then impregnated with 5% and 10% Fe (SF5Fe and SF10Fe) using an aqueous solution of iron sulfate heptahydrate ($FeSO_4{\cdot}7H_2O$) and sodium acetate (CH_3COONa), with the following proportions: 1.5 g SF/0.28 g $FeSO_4$/0.4 g CH_3COONa/5 mL H_2O. The solution was shacked in an ultrasonic bath and then heated under reflux. Finally, the solution was filtered and the solid was dried.[35]

The macroporosity of the foams was investigated using a mercury porosimeter. The specific surface area (BET), total pore volume (V_t), micropore and mesopore volumes (V_{micro} and V_{meso}) and the pore size distribution were determined using N_2 adsorption. Elemental analysis was carried out using a LECO CHN-2000 analyzer for C, H and N, and a LECO VTF-900 analyzer for direct oxygen determination. The morphology, distribution and particle size of the iron species were studied by scanning electron microscopy (SEM), whereas its crystalline structure was examined by X-ray diffraction (XRD).

2.3 Batch experiments

An incubation experiment was carried out using subsamples of soil with a 10% dose of foam using a total quantity of 20 g total mass per treatment as well as a control with untreated soil and washed sand in the same dose as the amendments. They were incubated in an orbital shaker at 170 rpm for 72 h and subsequently air-dried.

After soil incubation, EC and pH were measured following the methodology described in section 2.1.

The mobility and availability of As and Hg after batch experiments were evaluated by the TCLP test and the specific sequential extraction methods detailed in section 2.1.

Total and bioavailable PAH concentrations (C_T and C_B) were also determined after incubation experiments according to the methodology described in section 2.1, using 3 g of the amended soil.

2.4 Accuracy and precision of the analytical methods

Sample blanks were included through all stages of preparation and analysis. Triplicates were used to monitor analytical precision. Two certified reference soils, SRM 2709 and CRM170, were tested to monitor the accuracy of Hg, As and PAHs, respectively. The precision of the analysis was evaluated from the results of standard deviation (SD) and

relative standard deviations (% RSD). RSD values lower than 11% were found for all elements and compounds (Tables S1 and S2†).

2.5 Statistical analysis

The obtained data were statistically treated using SPSS version 24.0 for Windows. Analysis of variance (ANOVA) and test of homogeneity of variance were carried out. A *post hoc* least significant difference (LSD) test or Dunnett's T3 test was performed if there was homogeneity or no homogeneity, respectively.

3. Results and discussion

3.1 Amendment characterization

Sucrose carbon foams have a 3D open cellular structure mainly composed of macropores[45,46] (Fig. S1†). In this work, the sample was sieved at 0.2–0.5 mm for batch experiments; consequently a huge amount of macropores were partially destroyed (over 80%), but a fraction of pores in the range 20–1 μm was preserved (Fig. S2†). The nitrogen isotherms and pore size distribution of the raw SF and the impregnated SFs (SF5Fe and SF10Fe) are shown in Fig. S3.† All samples present type IV isotherms, with a well-defined capillary condensation step at p/p_0 ~0.6–0.8, evidencing the presence of a certain mesoporosity, while the nitrogen adsorbed at a low pressure range (p/p_0 <0.2) is related to microporosity.

Sample SF has a BET surface area and total pore volume of 306 $m^2\ g^{-1}$ and 0.24 $cm^3\ g^{-1}$, respectively, displaying a similar volume of micro- (0.13 $cm^3\ g^{-1}$) and mesopores (0.11 $cm^3\ g^{-1}$) (Table 1). It is to be expected that the impregnated foams will show a reduction in their textural properties with respect to the parent foam, being more pronounced as the percentage of the iron increases. However, the results shown in Table 1 and Fig. S3† suggest that the textural characteristics of the foams have not been compromised by the presence of the inorganic phase. Thus, similar pore volumes and pore size distributions are obtained in comparison with the raw SF, showing a wide distribution of mesopores in the range of 2–50 nm in all of them (Fig. S3†). In addition, the reduction in BET surface is rather slight, decreasing from 306 to 283 $m^2\ g^{-1}$ for SF5Fe and to 276 $m^2\ g^{-1}$ for SF10Fe (Table 1).

As can be seen in the SEM image (Fig. 1a), iron deposited on the surface of the sucrose foam had different morphologies, mainly in the form of nanoneedles, nanorods and pseudocubic crystals. The particle size for the different morphologies is shown in Fig. S4.† These morphologies are characteristic of the iron hydroxides (FeOOH) and magnetite (Fe_3O_4). XRD (Fig. 1b) also indicated the presence of FeOOH and Fe_xO_y (maghemite/magnetite). The results of the magnetic characterization (Fig. S5†) confirmed the presence of magnetite and not maghemite. The transition temperature at approximately 115 K, corresponding to the Verwey transition, is characteristic of magnetite.

Table 1 Textural properties of the sucrose foams

	S_{BET} ($m^2\ g^{-1}$)	V_t ($cm^3\ g^{-1}$)	V_{micro} ($cm^3\ g^{-1}$)	V_{meso} ($cm^3\ g^{-1}$)
SF	306	0.24	0.13	0.11
SF5Fe	283	0.23	0.12	0.11
SF10Fe	276	0.21	0.11	0.10

3.2 Soil analysis

The soils T and M showed pH and EC values of 7.44 ± 0.11 and 9.20 ± 0.02 and 0.43 ± 0.00 and 0.73 ± 0.04 dS m^{-1}, respectively. The T soil is characterized by its high concentrations of As (>5000 mg kg^{-1}) and Hg (>1000 mg kg^{-1}), whereas the M soil is characterized by its high concentrations of As (>2000 mg kg^{-1}) and PAHs (∑16 PAHs = 46 mg kg^{-1}). Both soils exceed the maximum levels permitted by regional and international regulations for metal(loid)s.[47–49] The total PAH concentration (∑16 PAHs) measured in the M soil also indicated a high level of contamination.[50] It is worth noting the differences found in As availability between both soils, being higher in soil M. Soil T and soil M show an availability of 8% (380 mg kg^{-1}) and 50% (1000 mg kg^{-1}), respectively. On the other hand, Hg availability in soil T (<0.1%) is much lower than As availability, as this element tends to be less mobile despite its high toxicity.

The concentration of PAH compounds grouped according to the number of rings (six- and five-member rings) in the M soil: 2/3-ring PAHs (Nap, Ace, Acy, Flu, Phe and Ant), 4-ring PAHs (Flt, Pyr, BaA and Chr), 5-ring PAHs (BbF, BkF, BaP, DahA), 6-ring PAHs (IcdP and BghiP), and individual PAHs are included in the ESI† (Fig. S6 and S7).

The most abundant PAHs found in the soil correspond to those with 4 and 5 rings, accounting for 82% of the total content. Among these compounds, benzo[*a*]pyrene (BaP) is considered one of the most toxic and carcinogenic PAHs and is often used as the main marker of soil pollution by PAHs.[51,52] Its concentration in the soil (4.41 ± 1.09 mg kg^{-1}) exceeds the maximum acceptable level stablished by Spain and other European countries. In addition, high contribution to the overall PAH content was found for the seven carcinogenic PAHs (∑7-car PAHs) (BaA, BaP, BbF, BkF, Chr, BghiP, IcdP) (25.01 ± 0.59 mg kg^{-1}), accounting for 55% of the total PAHs (Fig. S6a†).

As mentioned in the introduction, risk presented by hydrophobic organic contaminants in soils depends not only on the total concentration but also on their bioavailability, which is typically low in aged soils such as the one used in this study. The C_B determined on soil M after HPCD extraction was 17.63 ± 0.91 mg kg^{-1}, accounting for 38% of the concentration initially present in the soil. The results plotted in Fig. S6b† show that the heavier 6- and 5-ringed PAHs were the most bioavailable compounds (56% and 44%, respectively), while 4- and 2/3-ringed PAHs were less

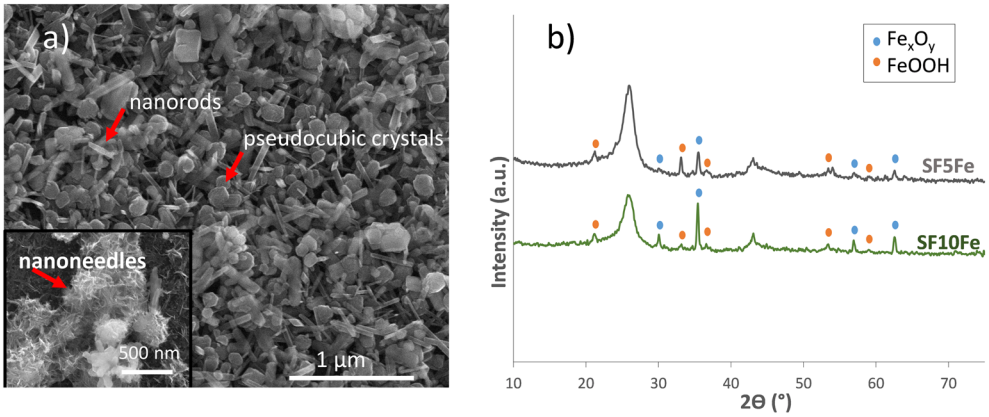

Fig. 1 (a) SEM image (detail of the nanoneedles at 500 nm) and (b) XRD pattern of SF5Fe and SF10Fe.

bioavailable, below 35% (Fig. S6b†). These results are consistent with the fact that lighter compounds experience aging processes to a greater extent than heavier compounds[53] as well as with their concentration, in such a way that compounds present less bioavailability as their concentration increases.[54] The C_B and C_R for individual PAHs are also presented in the ESI† (Fig. S7).

3.3 Effect of amendments on As and Hg availability (T soil)

The leachability of As was significantly reduced after the treatment with the SFs impregnated with iron nanoparticles (Fig. 2a). The impregnation with 10% Fe (SF10Fe) did not show higher efficiency than 5% Fe. The immobilization of As through adsorption and surface complexation on iron-based compounds is well known. In particular, iron hydroxides such as goethite (FeO(OH)) (Fig. 1) may favor As retention by sorption processes.[36]

The analysis of As speciation in the raw and treated T soil revealed that As is mainly associated with amorphous hydrous Fe oxides (70–71%) (Fig. 2b). The fraction of As extracted in the second step represented 17–18% of total As, providing an estimation of specifically sorbed As in the soil which may be mobilized due to changes in pH.[40] The concentration of As in the non-specifically bound, *i.e.*, the easily exchangeable As, was approximately 1%. In general, this fraction represents the one with the greatest environmental risk.

Table 2 shows pH and EC values together with the Fe concentration in TCLP extracts. In general, no changes in Fe leachability, pH and EC were observed after the addition of SFs.

When the availability of Hg was also studied in the T soil (Fig. 3a) it was found that the three treatments with SFs notably reduced Hg leachability. Immobilization percentages of 50–60%, irrespective of the foam used, were observed. The analysis of Hg speciation by the USEPA Method 3200 (Fig. 3b) revealed that most of the mercury in the raw and treated soil was extracted from the semi-mobile fraction, *i.e.*, Hg^{2+} complexes and/or Hg^0-metal amalgam.[41] Mercury was also found in the non-mobile fraction, *i.e.*, HgS. The percentage of

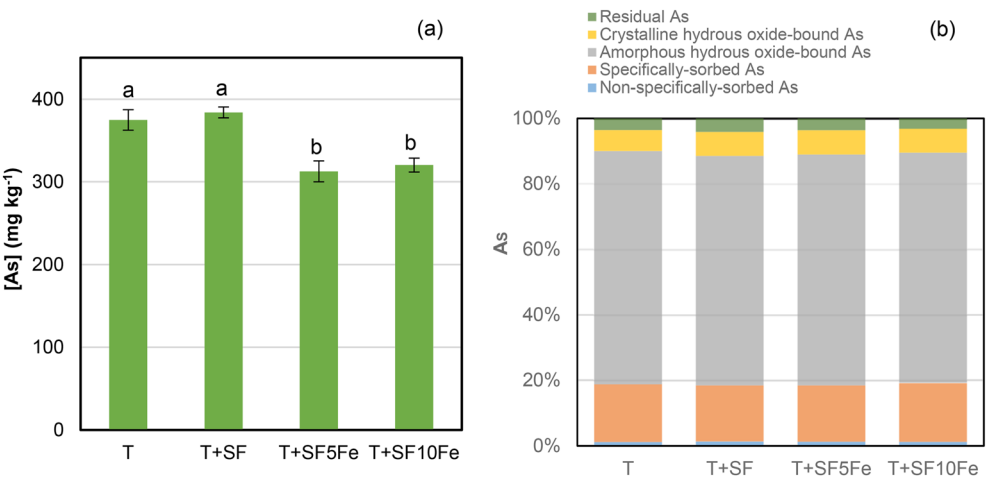

Fig. 2 (a) Concentration of As in TCLP extracts and (b) fractionation of As following an adopted sequential extraction method proposed by Wenzel *et al.*:[40] non-specifically sorbed As, specifically sorbed As, amorphous hydrous oxide-bound As, crystalline hydrous oxide-bound As and residual As in the untreated and treated T soil. Bars with the same letter do not differ significantly ($p < 0.05$).

Table 2 Concentration of Fe, pH and EC values in TCLP extracts in the untreated and treated T soil

	pH	EC (dS m^{-1})	Fe leachability (mg kg^{-1})
T	7.45 ± 0.03b	0.11 ± 0.02b	0.69 ± 0.09a
T + SF	7.71 ± 0.01a	0.11 ± 0.02b	0.45 ± 0.04a
T + SF5Fe	7.69 ± 0.09a	0.10 ± 0.01b	0.38 ± 0.18a
T + SF10Fe	7.72 ± 0.07a	0.16 ± 0.02a	0.75 ± 0.32a

For each column, samples with different letters indicate significant differences ($p < 0.05$). Standard deviation is represented by ±.

Hg in the semi-mobile fraction decreased after the treatment with SFs (Fig. 3b), which implied a lower leachability (Fig. 3a). The results suggest a lower availability of mercury bound to humic acid species[35] as a consequence of treatment with the SFs and their 3D structure composed of macro-, micro- and mesopores which favour the Hg adsorption (Table 1 and Fig. S2†).

The results show that the application of sucrose foams to this brownfield soil significantly reduced the availability of Hg in the soil. The effectiveness of the Hg immobilization is comparable to that achieved in a previous study using nZVI and carbon foams prepared from coal at a higher dose (20%) in the same soil.[35] Although the application of nZVI and similar nanocomposites can be more effective at reducing As availability than sucrose foams at 10% dose in this industrial soil, as seen in previous studies,[27] it should be considered that the As and Hg immobilization capacity using the sustainable material at lower doses is a key factor when considering a larger-scale remediation.

3.4 Effect of amendments on As and PAH availability (M soil)

Fig. 4 shows the As concentration in TCLP extracts in the untreated and treated M soil. The leachability of As was

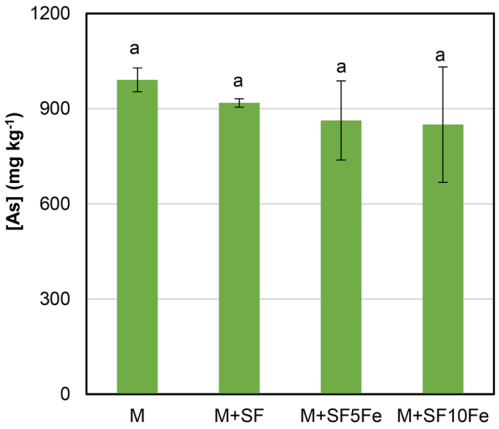

Fig. 4 Concentration of As in TCLP extracts in the untreated and treated M soil. Bars with the same letter do not differ significantly ($p < 0.05$).

slightly reduced after the treatment with the SFs impregnated with iron nanoparticles (SF5Fe and SF10Fe). As already mentioned, the immobilization of As may occur through adsorption and surface complexation on iron hydroxides such as goethite (FeO(OH)) (Fig. 1). However, the surface chemistry of FeO(OH) can vary with pH, which affects adsorption. In general, a lower pH enhances As immobilization. The electrostatic interactions between the negatively charged As oxyanions and the protonated groups of the Fe hydroxides are mainly favoured at the 4–8 pH range.[55] As can be observed in Table 3, the pH values in M soil are approximately 9.5, which led to a lower As immobilization.

In relation to the possible negative effects on EC soil values and Fe availability, the treatment with SFs, as in T soil, did not lead to significant changes on EC and the TCLP tests did not show an increase in available Fe (Table 3).

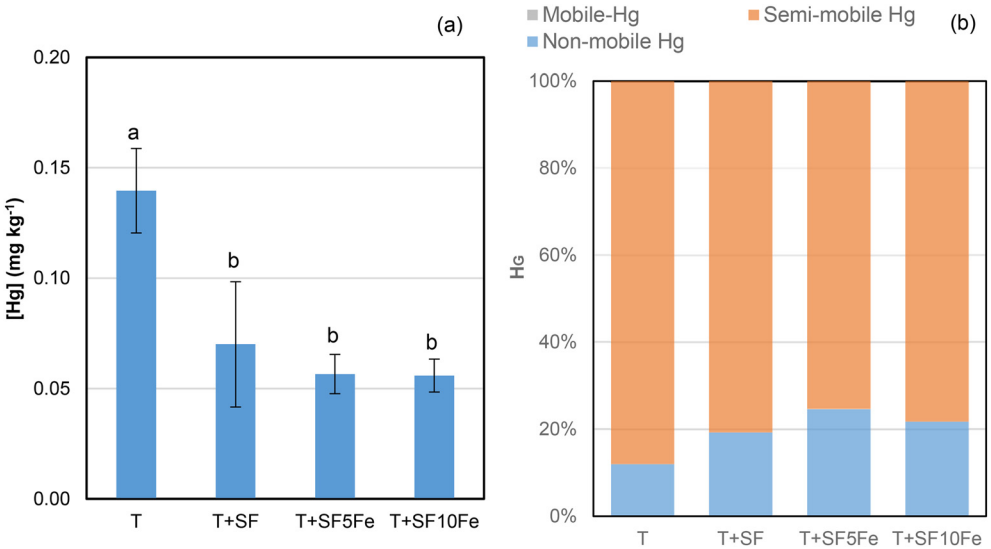

Fig. 3 (a) Concentration of Hg in TCLP extracts and (b) fractionation of Hg following the USEPA Method 3200: mobile Hg, semi-mobile Hg and non-mobile Hg in the untreated and treated T soil. Bars with the same letter do not differ significantly ($p < 0.05$).

Table 3 Concentration of Fe, pH and EC values in TCLP extracts in the untreated and treated M soil

	pH	EC (dS m^{-1})	Fe leachability (mg kg^{-1})
M	9.55 ± 0.03a	0.46 ± 0.01b	0.95 ± 0.09a
M + SF	9.49 ± 0.03a	0.46 ± 0.04b	0.83 ± 0.41a
M + SF5Fe	9.46 ± 0.07a	0.45 ± 0.01b	0.77 ± 0.45a
M + SF10Fe	9.48 ± 0.02a	0.57 ± 0.02a	0.46 ± 0.20a

For each column, samples with different letters indicate significant differences ($p < 0.05$). Standard deviation is represented by ±.

With the aim to determine if the incubation experiments may affect the PAH concentration, before evaluating the effect of the developed amendments on total and bioavailable PAH concentrations in M soil, exhaustive and non-exhaustive extractions were carried out on the control sample employed in batch experiments (untreated soil + sand) (M) as well as on the isolated amendment (SF) to study its potential risk. A reduction of 30% was determined on both total and bioavailable PAH content compared with the bulk sample (Fig. S8†). These results suggest that some biological degradation is likely to take place during incubation experiments as a consequence of shaking after reaching the water-holding capacity, so the results obtained for the amended soils were compared to this control sample. For the isolated amendments, the bioavailable fraction was below the analytical limit of detection and the total concentration was very low (≈1 mg kg^{-1}), identifying only low molecular weight PAHs (Fig. S8†). Therefore, it could be inferred that carbon foams did not represent a potential risk for soil in terms of PAH addition when compared with products such as some biochars.[56]

Fig. 5 compares the total PAH concentration found in the untreated and treated M soil. The treatment based on carbon foam amendments was highly effective for PAH immobilization. The C_T was reduced between 96% and 90% depending on the amendment. With regard to the PAH groups, the percentage of reduction was similar for all them. The huge reduction caused by the amendments can be attributed to the sorption properties of the carbonaceous amendment. The chemical structure of SFs is mainly composed of condensed aromatic sheets. Thus, π–π interactions between π electrons of aromatic rings in PAHs and π bonds are highly favorable, providing a relatively strong adsorption. In addition, the low H/C (≈0.14) and O/C (≈0.01) ratio of the SFs can improve hydrophobic interactions by intermolecular dipole–dipole interactions. It should be mentioned that apart from the iron species deposited by impregnation, the parent foam presents a small amount of iron oxide nanoparticles embedded in the carbon structure (0.3% wt.), which are introduced during foaming through the blowing agent.[46] These nanoparticles may be involved in π-complexation bonds with aromatic rings of PAHs. Apart from chemical characteristics, SFs also have a porous structure suitable for removing PAHs (Fig. S1†). Several studies have demonstrated that large-sized pores provide fast transfer paths for adsorption. Therefore, the presence of mesopores and macropores (Table 1 and Fig. S1 and S2†) in the SFs may improve the adsorption rate, whereas micropores (Table 1) act as active sites for PAH adsorption.[57] Although all the amendments led to a high reduction in the amount of total extractable PAHs, it can be observed that the amendment SF10Fe showed a minor reduction, with the differences being statistically significant for the ∑16PAHs in comparison with amendments SF and SF5Fe. These results suggest that the iron oxides/hydroxides on the surface of the carbon substrate may prevent the

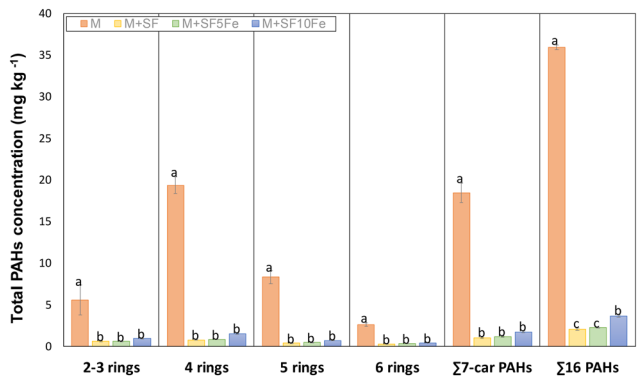

Fig. 5 Total PAH concentration of 2/3-ringed (2–3 rings), 4-ringed (4 rings), 5-ringed (5 rings), and 6-ringed (6 rings) in the untreated and treated M soil. Bars with the same letter do not differ significantly ($p <$ 0.05) within each PAH group.

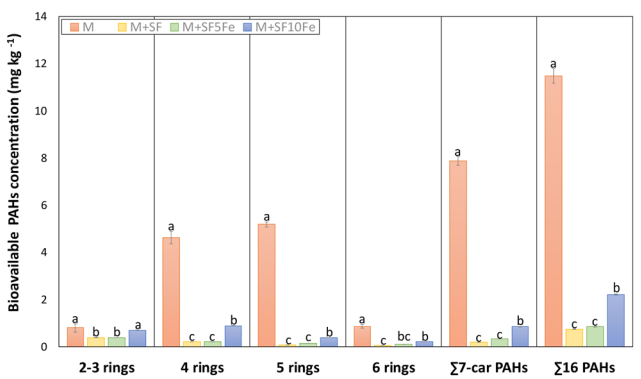

Fig. 6 Bioavailable PAH concentrations of 2/3-ringed (2–3 rings), 4-ringed (4 rings), 5-ringed (5 rings), and 6-ringed (6 rings) in the untreated and treated M soil. Bars with the same letter do not differ significantly ($p < 0.05$) within each PAH group.

adsorption of PAHs onto the carbon structure; however, π-complexation bonds may counteract this effect to a certain degree at low concentrations (≤5%).

With regard to the bioavailable fraction, the treatment with SFs also caused a significant decrease of PAH content, with the exception of the lightest compounds (2–3 rings) (Fig. 6). The reduction in the sum of 16 PAHs for the treated soils ranged from 94% to 82%, and similar reductions were observed for the sum 7-carcinogenic (97–88%). As can be observed in Fig. 6, a slight decrease in the sorption capacity was found in the soil treated with SF10Fe. This trend was similar to that found for total PAH concentration.

To better understand if the carbon-based amendments can modify PAH biodegradation, the ratio C_B/C_T was calculated for the treated soils (M + SF, M + SF5Fe, and M + SF10Fe) and compared with that obtained for the raw soil (M) (Fig. 7). For the sum of 16 PAHs, the addition of carbon foams SF and SF5Fe did not produce a significant change in the C_B/C_T, with values ranging from 0.32 to 0.38; however, this ratio was increased up to 0.61 for the soil treated with SF10Fe (Fig. 7), suggesting a higher mobility of contaminants and iron particles. On the other hand, several changes were produced in the C_B/C_T ratio when comparing the PAHs grouped by the number of rings. The control soil (M) showed the lowest value of C_B/C_T for 2–3 ringed compounds (0.18) and the highest for 5-ringed (0.62), whereas the opposite trend was observed for all the amended soils. Thus, the amended soils showed the highest C_B/C_T values (0.63–0.74) for the lightest compounds (2–3 ringed), and the lowest for 5-ringed compounds, the ratio for the amendment SF being significantly lower (0.19) (Fig. 7). This finding suggests that the heavier compounds which remained in the soil were less bioavailable than the lighter ones. These results also confirm that the carbon foam is the portion really reactive with the PAHs.

As occurred in the T soil, As leachability was slightly reduced with the application of sucrose foams at 10% dose. The basic character of the sucrose foams developed in this study (pH 9.0) must be taken into account unlike other carbon foams of acidic character (pH 4.2) previously used for As immobilization.[36] Nevertheless, sucrose foams are sustainable materials with controlled physicochemical properties for their use which would allow greater immobilization of As in field applications. Although the toxicity of nanoparticles is under discussion, As immobilization was found to be higher in a very similar soil using nZVI and magnetite and goethite nanoparticles.[17,28] In contrast, the application of the sucrose foams has led to a strong fixation of the organic compounds, achieving a great reduction in the amount of total extractable PAHs.[58] The effect of the studied amendments on the bioavailable fraction of PAHs was variable, which could facilitate the bioremediation or reduction of soil toxicity.

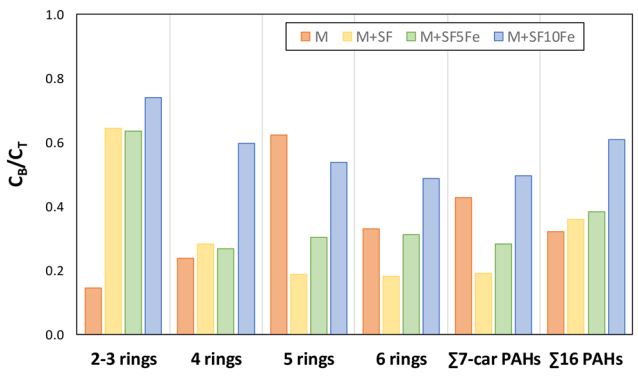

Fig. 7 Calculated ratio between the bioavailable concentration (C_B) and the total concentration (C_T) for the untreated and treated soils.

4. Conclusions

Several types of amendments have been used to immobilize metals and metalloids. However, some of them are capable of immobilizing metals but are not effective for immobilizing metalloids or can even mobilize them. The remediation becomes a greater challenge if the soil is polluted with metal(loid)s and organic compounds. The results of this study showed the efficiency of a new amendment based on biosustainable carbon foams for the immobilization of As in two soils co-contaminated with Hg and PAHs. Although further investigation will be carried out to determine the stability of the new amendments and to validate the results in other types of soils, the textural properties of the sucrose foams (macro-, meso- and microporosity), which could improve metal adsorption, their chemical structure (condensed aromatic sheets), which could favour PAH adsorption, and the possibility of depositing Fe nanoparticles (Fe_xO_y/FeO(OH)), which could favour metalloid adsorption, make them promising and versatile amendments for the remediation of multi-contaminated soils. In addition, the application of this nanocomposite did not affect the pH and EC or Fe availability in any of the soils tested. It should also be considered that the carbon foams developed in this study use a low-cost sustainable precursor with a low-energy cost preparation method that makes them an economically competitive material.

Author contributions

Íria Janeiro-Tato: methodology, investigation. Elena Rodríguez: conceptualization. Maria Antonia Lopez-Anton: writing – original draft, supervision, project administration, funding acquisition. Diego Baragaño: resources, validation. Laura Arrojo: formal analysis. Pilar Parra-Benito: methodology. Ana Isabel Peláez: writing – review & editing, supervision. José Luis R. Gallego: writing – review & editing, funding acquisition.

Conflicts of interest

There are no conflicts of interest to declare.

Acknowledgements

This work was funded by the research projects MCI-20-PID2019-106939GB-I00 (AEI/Spain, FEDER/EU), I+D+i PID2020-113558RB-C43/AEI/10.13039/501100011033 and IDI/2021/000031. The authors acknowledge the Government of the Principality of Asturias for the Severo Ochoa fellowship awarded to Iria Janeiro Tato (Ref.: BP21-108) and CSIC for the JAE-Intro ICU fellowship awarded to Laura Arrojo (Ref: JAEICU21-INCAR-63).

References

1 N. Rodríguez-Eugenio, M. McLaughlin and D. Pennock, *Soil Pollution: A Hidden Reality*, FAO, Rome, 2018, p. 142.
2 Y. Gong, D. Zhao and Q. Wang, *Water Res.*, 2018, 147.
3 B. González-Fernández, E. Rodríguez-Valdés, C. Boente, E. Menéndez-Casares, A. Fernández-Braña and J. R. Gallego, *Sci. Total Environ.*, 2018, **610–611**, 820–830.
4 Z. Sun, X. Xie, P. Wang, Y. Hu and H. Cheng, *Sci. Total Environ.*, 2018, **639**, 217–227.
5 Y. Xu, S. Dai, K. Meng, Y. Wang, W. Ren, L. Zhao, P. Christie and Y. Teng, *Sci. Total Environ.*, 2018, **630**, 618–629.
6 V. Antoniadis, S. M. Shaheen, E. Levizou, M. Shahid, N. K. Niazi, M. Vithanage, Y. S. Ok, N. Bolan and J. Rinklebe, *Environ. Int.*, 2019, **127**, 819–847.
7 A. Pratush, A. Kumar and Z. Hu, *Int. Microbiol.*, 2018, **21**, 97–106.
8 S. J. Connellan, *Respir. Med.*, 2017, **126**, 46–51.
9 B. Fernández, L. M. Lara, J. M. Menéndez-Aguado, J. Ayala, N. García-González, L. Salgado, A. Colina and J. L. R. Gallego, *Sci. Total Environ.*, 2020, **726**, 138546.
10 D. F. Hagmann, M. A. Kruge, M. Cheung, M. Mastalerz, J. L. R. Gallego, J. P. Singh, J. A. Krumins, X. N. Li and N. M. Goodey, *Sci. Total Environ.*, 2019, **690**, 1019–1034.
11 M. Kumar, N. S. Bolan, S. A. Hoang, A. D. Sawarkar, T. Jasemizad, B. Gao, S. Keerthanan, L. P. Padhye, L. Singh, S. Kumar, M. Vithanage, Y. Li, M. Zhang, M. B. Kirkham, A. Vinu and J. Rinklebe, *J. Hazard. Mater.*, 2021, **420**, 126534.
12 A. S. Ganie, S. Bano, N. Khan, S. Sultana, Z. Rehman, M. M. Rahman, S. Sabir, F. Coulon and M. Z. Khan, *Chemosphere*, 2021, **275**, 130065.
13 S. Ye, G. Zeng, H. Wu, C. Zhang, J. Liang, J. Dai, Z. Liu, W. Xiong, J. Wan, P. Xu and M. Cheng, *Crit. Rev. Environ. Sci. Technol.*, 2017, **47**, 1528–1553.
14 S. Zeng, Z. Dai, B. Ma, R. A. Dahlgren and J. Xu, *Earth Critical Zone*, 2024, **1**, 100002.
15 J. D. Aparicio, E. E. Raimondo, J. M. Saez, S. B. Costa-Gutierrez, A. Álvarez, C. S. Benimeli and M. A. Polti, *J. Environ. Chem. Eng.*, 2022, **10**, 107141.
16 K. N. Palansooriya, J. T. F. Wong, Y. Hashimoto, L. Huang, J. Rinklebe, S. X. Chang, N. Bolan, H. Wang and Y. S. Ok, *BioChar*, 2019, **1**, 3–22.
17 D. Baragaño, J. Alonso, J. R. Gallego, M. C. Lobo and M. Gil-Díaz, *Chemosphere*, 2020, **238**, 124624.
18 E. E. V. Chapman, C. Moore and L. M. Campbell, *Environ. Sci. Pollut. Res.*, 2020, **27**, 18757–18772.
19 E. Hiller, Ľ. Jurkovič, T. Faragó, M. Vítková, R. Tóth and M. Komárek, *Environ. Pollut.*, 2021, **285**, 117268.
20 H. Frick, S. Tardif, E. Kandeler, P. E. Holm and K. K. Brandt, *Sci. Total Environ.*, 2019, **655**, 414–422.
21 D. Baragaño, R. Forján, B. Fernández, J. Ayala, E. Afif and J. Gallego, *Environ. Sci. Pollut. Res.*, 2020, **27**, 33681–33691.
22 N. Bolan, A. Kunhikrishnan, R. Thangarajan, J. Kumpiene, J. Park, T. Makino, M. B. Kirkham and K. Scheckel, *J. Hazard. Mater.*, 2014, 266.
23 J. Xu, A. G. Bravo, A. Lagerkvist, S. Bertilsson, R. Sjöblom and J. Kumpiene, *Environ. Int.*, 2015, **74**, 42–53.
24 D. O'Connor, T. Peng, G. Li, S. Wang, L. Duan, J. Mulder, G. Cornelissen, Z. Cheng, S. Yang and D. Hou, *Sci. Total Environ.*, 2018, **621**, 819–826.
25 Z. Xiong, F. He, D. Zhao and M. O. Barnett, *Water Res.*, 2009, **43**, 5171–5179.
26 Y. Huang, M. Wang, Z. Li, Y. Gong and E. Y. Zeng, *J. Hazard. Mater.*, 2019, **373**, 783–790.
27 M. Gil-Díaz, E. Rodríguez-Valdés, J. Alonso, D. Baragaño, J. R. Gallego and M. C. Lobo, *Sci. Total Environ.*, 2019, **675**, 165–175.
28 D. Baragaño, J. Alonso, J. R. Gallego, M. C. Lobo and M. Gil-Díaz, *Chem. Eng. J.*, 2020, **399**, 125809.
29 F. Chen, M. Tan, J. Ma, S. Zhang, G. Li and J. Qu, *J. Hazard. Mater.*, 2016, **302**, 250–261.
30 Y. Ma, X. Li, H. Mao, B. Wang and P. Wang, *Chem. Eng. J.*, 2018, **353**, 410–418.
31 A. Cristaldi, G. O. Conti, E. H. Jho, P. Zuccarello, A. Grasso, C. Copat and M. Ferrante, *Environ. Technol. Innovation*, 2017, **8**, 309–326.
32 G. Devendrapandi, X. Liu, R. Balu, R. Ayyamperumal, M. Valan Arasu, M. Lavanya, V. R. Minnam Reddy, W. K. Kim and P. C. Karthika, *Environ. Res.*, 2024, **249**, 118404.
33 B. Zhang, Y. Guo, J. Huo, H. Xie, C. Xu and S. Liang, *Chem. Eng. J.*, 2020, **382**, 123055.
34 V. Mesa, A. Navazas, R. González-Gil, A. González, N. Weyens, B. Lauga, J. L. R. Gallego, J. Sánchez and A. I. Peláez, *Appl. Environ. Microbiol.*, 2017, **83**, e03411-16.
35 I. Janeiro-Tato, M. A. Lopez-Anton, D. Baragaño, C. Antuña-Nieto, E. Rodríguez, A. I. Peláez, J. R. Gallego and M. R. Martínez-Tarazona, *Environ. Sci. Eur.*, 2021, **33**, 127.
36 I. Janeiro-Tato, D. Baragaño, M. A. Lopez-Anton, E. Rodríguez, A. I. Peláez, R. García and J. R. Gallego, *Chemosphere*, 2022, **301**, 134645.
37 H. Liu, S. Wu, N. Tian, F. Yan, C. You and Y. Yang, *J. Mater. Chem. A*, 2020, **8**, 23699–23723.
38 J. R. Gallego, N. Esquinas, E. Rodríguez-Valdés, J. M. Menéndez-Aguado and C. Sierra, *J. Hazard. Mater.*, 2015, **300**, 561–571.
39 USEPA, *SW-846 Test Methods Eval. Solid Waste, Phys. Methods*, 1992.
40 W. W. Wenzel, N. Kirchbaumer, T. Prohaska, G. Stingeder, E. Lombi and D. C. Adriano, *Anal. Chim. Acta*, 2001, **436**, 309–323.

41 USEPA, *Method 3200: Mercury Species Fractionation and Quantification by Microwave Assisted Extraction, Selective Solvent Extraction and/or Solid Phase Extraction*, moz-extension://09095646-0d3d-433f-8839-0c59dfcfb1ad/enhanced-reader.html?openApp&pdf=https%3A%2F%2Fwww.epa.gov%2Fsites%2Fproduction%2Ffiles%2F2015-12%2Fdocuments%2F3200.pdf, (accessed 26 March 2021).
42 L. Beesley, E. Moreno-Jiménez and J. L. Gomez-Eyles, *Environ. Pollut.*, 2010, **158**, 2282–2287.
43 J. L. Gomez-Eyles, M. T. O. Jonker, M. E. Hodson and C. D. Collins, *Environ. Sci. Technol.*, 2012, **46**, 962–969.
44 M. Kołtowski, I. Hilber, T. D. Bucheli, B. Charmas, J. Skubiszewska-Zięba and P. Oleszczuk, *Chem. Eng. J.*, 2017, **310**, 33–40.
45 L. López-Toyos, M. A. López-Antón, E. Rodríguez, R. García and M. R. Martínez-Tarazona, *Fuel*, 2023, **345**, 128181.
46 R. García, E. Rodríguez, M. A. Díez, A. Arenillas, S. F. Villanueva, N. Rey-Raap, C. Cuesta, M. A. López-Antón and M. R. Martínez-Tarazona, *Materials*, 2023, **16**, 1336.
47 T. Crommentuijn, D. Sijm, J. De Bruijn, M. Van den Hoop, K. Van Leeuwen and E. Van de Plassche, *J. Environ. Manage.*, 2000, **60**, 121–143.
48 MEF, *Ministry of Environment Finland, Government Decree on the Assessment of soil contamination and remediation needs 214/2007*, March 1, 2007.
49 BOPA, Boletín Oficial del Principado de Asturias, *Generic reference levels for heavy metals in soils from Principality of Asturias*, Spain, 2014, **http://sede.asturias.es/bopa/2014/04/21/2014-06617.pdf**.
50 T. Liu, Z. Xiong, P. Ni, Z. Ma, Y. Tan, Z. Li, S. Deng, Y. Li, Q. Yang and H. Zhang, *Chem. Eng. J.*, 2023, **454**, 140095.
51 S. N. Sushkova, T. M. Minkina, S. S. Mandzhieva, G. K. Vasilyeva, N. I. Borisenko, I. G. Turina, O. V. Bolotova, T. V. Varduni and R. Kızılkaya, *J. Soils Sediments*, 2016, **16**, 1323–1329.
52 H. Tan, Q. Wu, C. Wang, D. Wu, Y. Cui, Q. Li and C. Wu, *Chemosphere*, 2022, **306**, 135556.
53 J. L. Gomez-Eyles, C. D. Collins and M. E. Hodson, *Environ. Pollut.*, 2010, **158**, 278–284.
54 S. P. Maletić, J. M. Beljin, S. D. Rončević, M. G. Grgić and B. D. Dalmacija, *J. Hazard. Mater.*, 2019, **365**, 467–482.
55 E. Mele, E. Donner, A. L. Juhasz, G. Brunetti, E. Smith, A. R. Betts, P. Castaldi, S. Deiana, K. G. Scheckel and E. Lombi, *Environ. Sci. Technol.*, 2015, **49**, 13501–13509.
56 S. E. Hale, J. Lehmann, D. Rutherford, A. R. Zimmerman, R. T. Bachmann, V. Shitumbanuma, A. O'Toole, K. L. Sundqvist, H. P. H. Arp and G. Cornelissen, *Environ. Sci. Technol.*, 2012, **46**, 2830–2838.
57 F. Li, J. Chen, X. Hu, F. He, E. Bean, D. C. W. Tsang, Y. S. Ok and B. Gao, *J. Cleaner Prod.*, 2020, **255**, 120263.
58 M. Boulangé, C. Lorgeoux, C. Biache, J. Michel, R. Michels and P. Faure, *Environ. Sci. Pollut. Res.*, 2019, **26**, 1693–1705.